P-5: Self-Release Nickel Induced Lateral Crystallized (SR-NILC) Low Temperature Polycrystalline Silicon Films and Thin Film Transistors

Shuyun Zhao[1], Zhaojun Liu[1], Zhou Wei[1], Zhiguo Meng[1,2], Man Wong[1] and Hoi Sing Kwok [1]*

[1]Department of Electronic and Computer Engineering, Hong Kong University of Science and Technology, Clear Water Bay, Kowloon, Hong Kong

[2]Inst. Of Opto-electronics, School of Information, Nankai University, Tianjin 300071, PR China

ABSTRACT

Nickel induced crystallization of a-Si with a self-release inducing source was studied. Three main factors affecting the crystallization rate were investigated. The new source possesses an effect of nickel self-release and the crystallized poly-Si has obviously lower nickel residua. The p-channel thin film transistors (TFTs) based on the SR-NILC poly-Si film showed lower off-state current (I_{off}) and gate induced drain leakage (GIDL).

1. Introduction

While most active matrix liquid crystal displays (AM-LCD) are made of amorphous silicon (a-Si) thin film transistors (TFT), there is always a demand for polycrystalline silicon (poly-Si) based active matrix displays because the latter can provide much higher resolution and smaller pixels. As well, some of the driver circuitry can be integrated onto the glass substrate in the case of poly-Si TFT. Additionally, poly-Si TFT is more stable than a-Si TFT in terms of driving organic light emitting diode (OLED) displays. Thus low cost, high performance and reliable low temperature poly-Si (LTPS) processing technologies are greatly required [1].

Currently, the polycrystalline silicon (poly-Si) film is obtained mainly by methods of solid-phase crystallization (SPC) [2], excimer laser annealing (ELA) [3], rapid thermal annealing (RTA) [4] and metal-induced lateral crystallization (MILC) [5] technology. Poly-Si film obtained by MILC with the merits of high uniformity and low cost has attracted much considerable attention [6].

Normally the optimum inducing metal Ni is formed by evaporation or sputtering of pure Ni. Thus prepared poly-Si contains comparatively high concentration of nickel residua with the ratio of Ni/Si at an order of magnitude of $\sim 10^{-3}$ [6]. The investigation on MILC poly-Si has been trended to pay more attention on how to decrease the residual nickel concentration. There have been several attempts to reduce the Ni content in MIC based TFT. Giant grain silicon (GGS) has been obtained by Ni-mediated crystallization of a-Si with a silicon-nitride (SiNx) cap layer [7] or using solution based metal-induced crystallization (SMIC) [1]. In this paper, a new kind of inducing source has been proposed, and the mechanism of its effective depression of the Ni residua in crystallized poly-Si is discussed.

2. Experiment

The fabrication process began with 4-inch c-Si wafers covered with 500nm thermal oxide. Then 50nm a-Si active layer was deposited by low-pressure chemical vapor deposition (LPCVD). After that, a 100nm-thick low-temperature oxide (LTO) was deposited. By using photolithography and etching process, this LTO layer was patterned to form various opening lines with different width and space, which we called inducing lines (IL), as shown in Figure 1. Finally, Self-Release (SR) Ni/Si oxide source was sputtered on the sample surface. The target we used was an alloy of nickel and silicon with a component ratio of Ni:Si=1:9, and the sputtering is operated in ambience of argon mixed with oxygen with the ratio of 200:1. For comparison, 5nm pure nickel deposited sample was also prepared using e-beam evaporation, which was normally used in MILC.

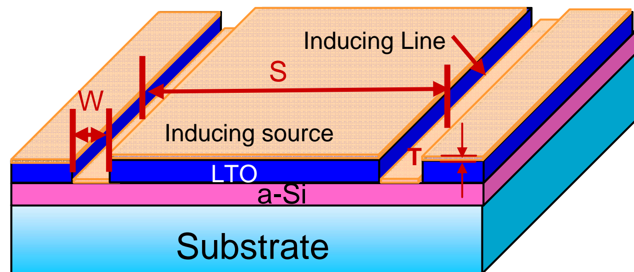

Figure 1. The schematic of the SR-NILC system.

After Ni or SR-Ni/Si oxide deposition, the samples were annealed in nitrogen atmosphere at the temperature of 590ºC for 1 hour to conduct the crystallization of a-Si. During the crystallization process, the width (W) of inducing line (IL), the space (S) between inducing lines (IL) and the thickness (T) of sputtered inducing source all affected the crystallization rate under certain temperature. Figure 1 shows the schematic of this system after SR-Ni/Si oxide deposition, where the W, S and T were labeled. Detailed results will be discussed in the later part of the paper. The residual nickel concentration of the resulted poly-Si thin films prepared with the two kinds of sources were compared and characterized by TOF-SIMS. The component of the inducing source was analyzed using XPS. P-type TFTs were fabricated with the Ni-Si oxide source and their performances were characterized.

 ISSN/009-0966X/09/3903-1096-$1.00 © 2009 SID

3. Results and discussion

3.1 The effect of SR-Ni/Si oxide thickness (T)

In this particular crystallization structure, the crystallization normally begins in the a-Si underneath the IL and laterally grows with the annealing time, as shown in Figure 2. The crystallization direction is perpendicular to the inducing line except the end of the line which will not be discussed in this paper. Crystallization rate is the lateral growth length of the Ni-induced poly-Si during a period of time, which equals to 1 hour in this session.

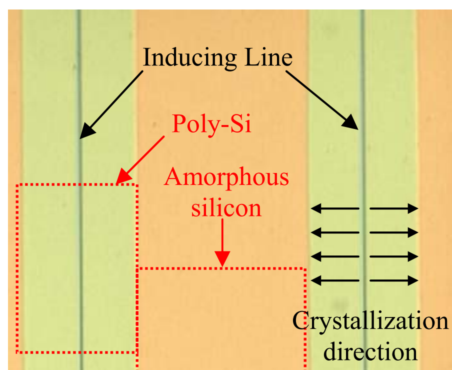

Figure 2. **Microscope photo of the partially crystallized sample after annealed at 590ºC for 1hour**

Figure 3 shows the crystallization rate vs. thickness of inducing source under the same annealing condition. Here, the width and space of IL were 30μm and 5000 μm respectively. It should be noticed that the effective Ni thickness of SR-Ni/Si oxide source is the real thickness divided by a factor of 10.

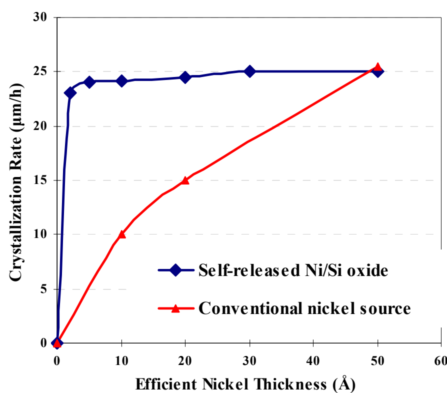

Figure 3. Crystallization rate as a function of efficient nickel thickness of two kind of nickel source layer

The relationship of the crystallization rate with the thickness of two inducing sources is quite different. For the SR-Ni/Si oxide source, the crystallization rate reached a constant when the thickness is more than 4Å. But for pure Ni source, the rate varied with the thickness obviously. That means that the process tolerance of SR-Ni/Si oxide source is better than that of pure Ni metal.

3.2 The effect of width of IL (W)

Figure 4 shows the crystallization rate as a function of the width of IL. The width of inducing line changes from 2μm to 30μm. Here, the space between lines is fixed at 60 μm. The Ni-Si oxide was sputtered with a DC power of 7W for 3min, which provided a thickness of 2nm. From Figure 4, we can see that, with the W increasing, the crystallization rate increases firstly and then saturated when the W is larger than 8μm. That's because the crystallization needs a certain quantity of nickel to make the "front" move laterally. The area directly contact with the a-Si surface is determined by the width of IL. Under a certain sputtering condition, larger contact area to a-Si means more nickel diffusion into the a-Si film and gives larger crystallization rate. At a certain temperature, the crystallization rate increases with increasing nickel concentration in a-Si until it reaches the saturation rate. So, when the W is smaller than 8μm, there is not enough nickel diffused into a-Si and does not reach the saturation rate. When the W is larger than 8μm, with S fixed at 60 μm, the nickel diffused into a-Si is enough to form a smooth "front" and saturated at 590 ºC. Additional nickel diffused into the a-Si will not affect to the crystallization rate any more. Another very interesting phenomenon was observed, which is shown in Figure 5. Figure 5 shows a micro-scope photo of the sample after annealing at 590ºC for 0.5hour with the W of 1 μm and 2 μm respectively. As shown in Figure 5, the width of inducing line (W) is 1 μm for the top part of the figure, and the W for the part below dot line is 2 μm. This phenomenon shows that when the W of IL is smaller than 2 μm, with the space (S) fixed at 60 μm, the nickel diffused into a-Si film was not enough for the formation of a smooth "crystallization front line". So only some disk-like crystallized poly-Si domain was distributed along the inducing line.

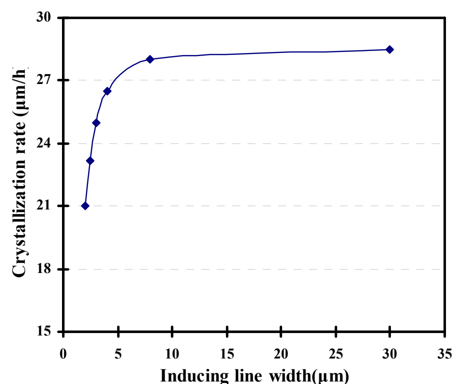

Figure 4. Crystallization rate as a function of the width of inducing line (W).

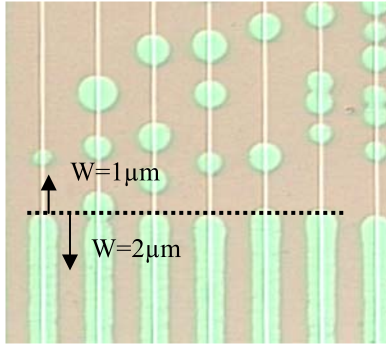

Figure 5. The micro-scope photo of the sample after annealing at 590ºC for 0.5 hour

3.3 The effect of space between IL (S)

Not only the thickness of inducing source (T) and the width of inducing line (W), but also the space between inducing lines (S) affects the crystallization rate. Figure 6 shows the crystallization rate as a function of S with the W of 6 μm and T of 2nm. When W and T are fixed, the smaller S, the more IL is distributed in a certain area. So, more nickel will diffuse into the a-Si and give a faster crystallization rate. As mentioned previously, if the diffused nickel is rich enough for smooth "front" and reach the saturated crystallization rate, there will be no further increasing of crystallization rate with decreasing S. From Figure 6, we can find that, when S is larger than 60 μm, the crystallization rate decrease with the S increasing. That's because with the ratio of W/S decreasing, the nickel diffused into a-Si film decreases, which lower the crystallization rate.

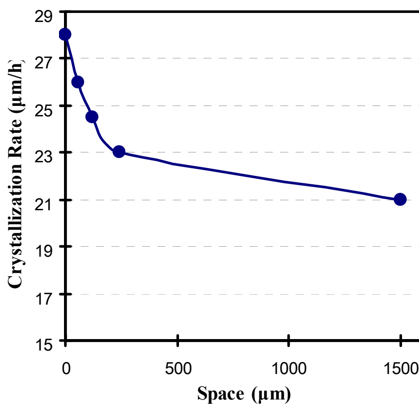

Figure 6. The crystallization rate as a function of the space between the IL (S) with a fixed W.

After all these investigations, we found that the S really affected the crystallization rate and the influence changes with W. More detailed and numerical study will be performed in future.

3.4 Components analysis of this self-release source

The components in Ni-Si oxide source were analyzed by X-ray photoelectron spectroscopy (XPS). As shown in Figure 7, the peaks at the binding energies of 854.3eV, 532.5eVand 103.5eV correspond to the amount of Ni_{2p}, O_{1s} ad Si_{2p}, respectively. It implies that Si and Ni atoms are surrounded by oxygen atoms. The ratio of atom concentration of O, Si and Ni is 64.18:34.19:1.63 (i.e. 40:21:1), as shown in Figure 7. It should be noticed that the target we used was nickel and silicon alloy with the ratio of Si:Ni=9:1. The sputtered process was performed in ambience of argon mixed with oxygen with the ratio of 200:1. So we would like to suppose that sputtered Ni/Si alloy film would be a $19SiO_2$:Si_2NiO_2 alloy structure. The Si_2NiO_2 probably consists of Si_2O-NiO mixed structure and its molecular concentration is just 5% in the sputtered Ni/Si oxide. As all have known [8], the bond strength of Ni-O is just 93.6±0.9 K car/mol, which is lower than that of Si-O (190.9±2 K car/mol) but higher than one of Si-Ni (76±4 K car/mol) [8]. By inter-comparing these bond strengths, we suggest the induced crystallization mechanism could be: the Si atom in a-Si neighboring with the Ni-Si oxide has ability to despoil the Ni from the Si_2O-NiO, which is self-oxide as SiO_2 and releases a monatomic Ni. This reaction can be described as $NiO+Si_2O \rightarrow 2SiO+Ni$. At the same time, the release Ni atom will react with Si in a-Si to form Ni-silicide as the crystallization media to induce crystallization of a-Si sequentially.

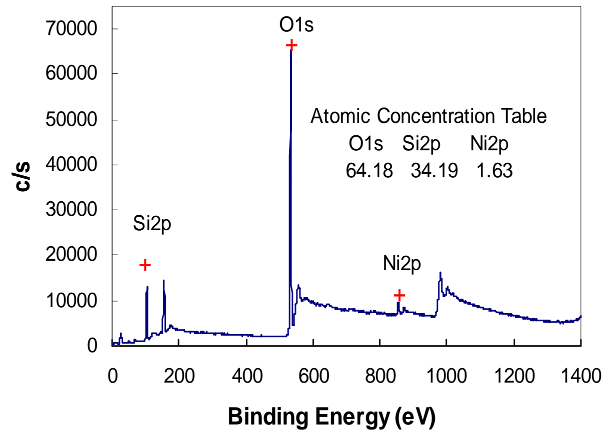

Figure 7. XPS spectrum of SR inducing source.

In this crystallization process, SR-Ni/Si oxide source just act as a supplement source of Ni at a relatively slow rate. This kind of Ni-induce source tardily provides Ni by reaction of Si with Ni-Si oxide, which is different from the pure Ni source which provides abundant pure Ni atoms. So nickel consumption in the nickel oxide will be less than that pure source. This self-release reactive Ni can decrease Ni residua in poly-Si.

3.5 Nickel concentration analysis by SIMS

In order to study the process tolerance and compare the performances of crystallized poly-Si, we prepared three different nickel sources on the same amorphous silicon precursor called samples A, B and C, respectively. Sample A was sputtered with power of 7W for 3 minutes, sample B was sputtered with power of 7W for 60 minutes, sample C is the pure nickel deposited by e-beam evaporation with the thickness of 50Å. Then three samples were fully crystallized to poly-Si by annealing at 590ºC for 2 hours.

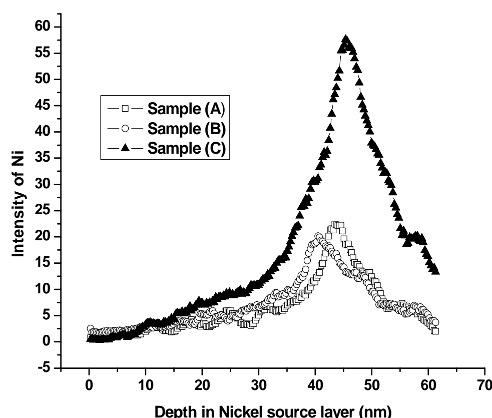

Figure 8. **nickel distributions in three samples**

The residual Ni distribution in three crystallized poly-Si were measured near inducing hole along the film depth vertical to film surface by TOF-SIMS, as shown in Figure 8. Their distribution in three samples is not uniform. The peak of nickel residua is close to bottom of a-Si near glass and the Ni residua in sample A and B is almost same but lower than that in sample C by half of order of magnitude. It implies that thickness of inducing source is not as effective to affect Ni residua as the initial nickel content at the interface neighboring a-Si film.

3.6 Performance of poly-Si TFT

Figure 9 shows transfer characteristics of p-channel poly-Si TFTs, which were made with poly-Si crystallized by SR-Ni/Si oxide source and by pure Ni source. The devices were fabricated with a W/L ratio of 30μm/10μm and a 50nm gate insulator layer. As we can see, the mainly merit of the Ni/Si oxide is to decrease the off-state current (I_{off}) and the gate-induced drain leakage current (GIDL). Comparing with sample C, I_{off} and GIDL is four times lower than those of sample C. The improvement is consistent with lower residual nickel content in poly-Si shown in Figure 8.

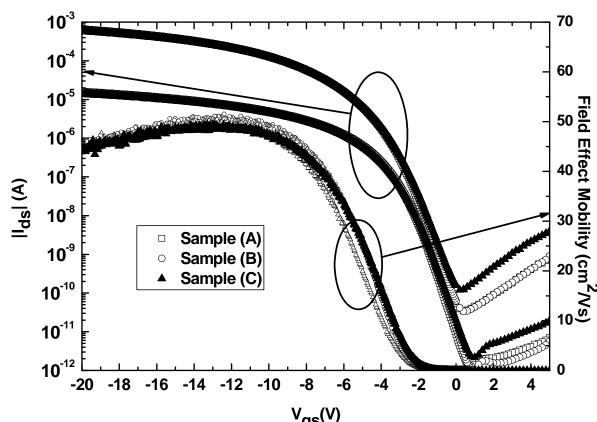

Figure 9. **Transfer characteristics and μ_{FE} of three types of TFTs. (a) sputtering 3'(b) sputtering 1hr (c) e-beam 50 Å**

4. Conclusion

We have developed a new type of SR-Ni/Si oxide source suitable for MILC poly-Si preparation. With this kind of nickel source, the nickel residua in poly-Si film were efficiently reduced, the leakage current of poly-Si TFT was reduced consequently. It has better tolerance for prepared poly-Si materials and TFTs. This SR- Ni/Si oxide source provides a wider process window and can prevent the effect of the variation of process parameters between batches on poly-Si TFTs .

5. Acknowledgments

This work was partly supported by China's NSFC Key Project (Grant No. 60437030) and the Hong Kong Government Innovation and Technology Fund.

6. Reference

[1] Z. Meng. S. Zhao, C. Wu, B. Zhang. M. Mong and H. S. Kwok, Journal of Display Technology, vol. 2, No. 3, pp265-273.

[2] C.H. Hong, C.Y. Park, H. J. Kim, J. Appl. Phys. 71, 5427(1992).

[3] Y.-H. Kim, C.-H. Chung, S. J. Yun, J. Moon, D.-J. Park, D.-W. Kim, J.W. Lim, Y.-H. Song, J. H. Lee, Thin Solid Films 493, 192 (2005).

[4] S. H. Jung, H. K. Lee, C. Y. Kim, S. Y. Yoon, C. D. Kim and I. B. Kang, SID 08 DIGEST. 101 (2008)

[5] C. Y. Yuen, M. C. Poon, W. Y. Chan and M. Qin, J. Appl. Phys. 92, 6291 (2002).

[6] M. Wang, and M. Wong, IEEE Trans. Electron Devices, 48,1655 (2001)

[7] J. H. Choi, J. H. Cheon, S. K. Kim and J. Jang. Displays, vol. 26, pp. 137–142, 2005

[8] Handbook of Chemistry and Physics, 60th, p.F-220, CRC PRESS. INC. (1980)